

A Generalized Method for Computing Oscillator Phase Noise Spectra

Piet Vanassche, Georges Gielen and Willy Sansen
Katholieke Universiteit Leuven - ESAT/MICAS
Kasteelpark Arenberg 10, B-3001 Leuven, Belgium
georges.gielen@esat.kuleuven.ac.be

ABSTRACT

This paper presents a generalized semi-analytic method for computing oscillator phase noise spectra, including the details very close to the oscillation frequency. The starting point is a general relation between an oscillator's output power spectral density and the characteristics of the input noise processes. For weak input noise processes that vary sufficiently fast over time, this relation reduces to an analytic expression. For cases that do not satisfy these conditions, the relation is, in part, evaluated numerically. This is accomplished using techniques for exponential data fitting. The resulting method is able to compute oscillator phase noise spectra for a wide range of input noise characteristics.

1. INTRODUCTION

Oscillators are key building blocks in almost all of today's communication systems. One of the most important quality measures for an oscillator involves their phase noise behavior. This stochastic phase behavior is characterized through the power spectral density (PSD) of the oscillator's output signal—which, in this text, is also referred to as the oscillator's *phase noise spectrum*. Design requirements concerning the quality of an oscillator are often specified as constraints on the spectral spreading of this PSD. Hence, it is important to provide designers with methods to compute them.

Computing an oscillator's PSD involves solving three problems:

1. Identify and characterize the input noise processes disturbing the oscillator's behavior. In this area, especially the characterization of $1/f$ noise is still an open problem [1] although some acceptable models have been presented [2, 3].
2. Given the input noise processes, extract the equations governing the oscillator's stochastic phase behavior. This particular problem has received much attention in recent years [3, 4, 5, 6] and is considered to be solved.
3. Given the phase behavior, find the oscillator's output PSD. Up to now, this problem only received limited attention. In [5], expressions are presented based on small-signal assumptions. However, as pointed out in [4], small-signal assumptions do not apply to oscillators. In [3, 4], an analytic expression is presented for oscillator spectra in the presence of *white* input noise. This work also contains two separate asymptotic approximations for, respectively, the very close-in phase noise spectrum and for the spectrum far away from the oscillation frequency. The approximations are based on the work in [7, 8]. They are claimed to hold for both white and colored input noise.

The work in this paper focuses on solving the third problem. As a starting point, we develop a general relation between an oscillator's

Permission to make digital or hard copies of all or part of this work for personal or classroom use is granted without fee provided that copies are not made or distributed for profit or commercial advantage and that copies bear this notice and the full citation on the first page. To copy otherwise, to republish, to post on servers or to redistribute to lists, requires prior specific permission and/or a fee.

ICCAD '03, November 11-13, 2003, San Jose, California, USA.

Copyright 2003 ACM 1-58113-762-1/03/0011 ...\$5.00.

output PSD and the input noise characteristics. For weak noise sources that vary sufficiently fast over time, this relation reduces to a single analytic approximation that combines both the asymptotes from [3]. For other types of noise processes, we refine results using numerical techniques based on exponential data fitting [9].

The remainder of this paper is structured as follows. Section 2 summarizes theory that is needed to characterize an oscillator's stochastic phase behavior (the second step as mentioned above). Next, section 3 reviews some general results on the spectra of phase-modulated periodic signals. In section 4, these results make up the starting point for elaborating a general relation between an oscillator's output PSD and the input noise characteristics. Here, we also consider analytic approximations for weak and fast-varying input noise processes. Section 5 discusses a numerical method that can be used when these approximations break down. Results identifying the range of validity of the traditional $1/f^2-1/f^3$ phase noise characteristic are presented in section 6. Finally, conclusions are drawn in section 7.

2. AVERAGED STOCHASTIC PHASE BEHAVIOR

The behavior of an oscillator perturbed by a noise source $\epsilon n(t)$ —with ϵ denoting the strength (standard deviation) of the noise source— can be modeled as [2, 4]

$$x(t) = x_s(t + \theta(t)) + \Delta x(t) . \quad (1)$$

Here, $x(t)$ represents the output of the noisy oscillator while $x_s(t)$ models the T -periodic steady-state behavior of the noise-free system. Furthermore, the process $\theta(t)$ captures the oscillator's phase behavior. The term $\Delta x(t)$ represents a small orbital deviation. Since the latter term has no part in the spectral spreading of the oscillator's output PSD, it is neglected in the analysis that follows.

For a sufficiently weak noise source $\epsilon n(t)$, i.e. for a noise strength $\epsilon \ll 1$, it is shown in [2, 3, 4] that the phase behavior $\theta(t)$ is related to the driving noise process $\epsilon n(t)$ by

$$\frac{d\theta}{dt} = \epsilon \Gamma(t + \theta) n(t) . \quad (2)$$

Here, $n(t)$ is the normalized input noise process with ϵ denoting the noise strength. Furthermore, $\Gamma(t)$ is the corresponding $-T$ -periodic—impulse sensitivity function (ISF) [5]. A rigorous method to compute this ISF requires us to project the noise, i.e. the perturbations, onto the oscillator's orbit using the perturbation projection vector [3, 4].

Assuming $n(t)$ to be stationary and Gaussian, it was recently shown [6] that, up to first order in ϵ , (2) can be reduced to

$$\frac{d\theta}{dt} = \varepsilon \bar{n}(t). \quad (3)$$

Here, $\bar{n}(t)$ is called the —normalized— *averaged input noise*. This noise can be shown to be both stationary and Gaussian with its autocorrelation function equaling

$$\Phi_{\bar{n}}(\tau) = E \{ \bar{n}(t + \tau) \bar{n}(t) \} \quad (4)$$

$$\approx \frac{1}{T} \int_{-\frac{T}{2}}^{\frac{T}{2}} \Gamma(t + \frac{\tau}{2}) \Gamma(t - \frac{\tau}{2}) \Phi_n(\tau) dt \quad (5)$$

where $\Phi_n(\tau) = E \{ n(t + \tau) n(t) \}$ is the autocorrelation function corresponding to the original noise source $n(t)$. Observing (5), it is seen that averaging removed θ from the right-hand side of the equation (2). This greatly simplifies further analysis.

With $\bar{n}(t)$ Gaussian, the same will hold for the phase differences $\theta(t + \tau) - \theta(t) = \int_t^{t+\tau} \bar{n}(s) ds$. As will be seen in the next section, the variance of these phase differences, i.e.

$$\sigma^2(\tau) = E \left\{ (\theta(t + \tau) - \theta(t))^2 \right\}, \quad (6)$$

is the quantity of greatest interest in finding the oscillator phase noise spectrum. It can be shown that this variance satisfies

$$\frac{d^2}{d\tau^2} \sigma^2(\tau) = \varepsilon^2 2 \Phi_{\bar{n}}(\tau), \text{ with } \sigma^2(0) = 0, \frac{d}{d\tau} \sigma^2(0) = 0. \quad (7)$$

As an important property of $\sigma^2(\tau)$, it holds that for $\tau > \tau_{noise}$

$$\frac{d}{d\tau} \sigma^2(\tau) \approx \varepsilon^2 2 \int_0^{\infty} \Phi_{\bar{n}} ds = \varepsilon^2 S_{\bar{n}}(0) = \text{constant}. \quad (8)$$

Here, τ_{noise} is the time constant of the input noise, i.e. the time constant beyond which $\Phi_{\bar{n}}(\tau) \approx 0$. Furthermore,

$$S_{\bar{n}}(\omega) = \int_{-\infty}^{+\infty} \Phi_{\bar{n}}(\tau) e^{-j\omega\tau} d\tau \quad (9)$$

is the PSD of the —normalized— averaged input noise signal $\bar{n}(t)$. Having established these results, we can go on computing the oscillator's output PSD.

3. PHASE-MODULATED OSCILLATOR SPECTRA

An oscillator's output PSD $S_x(\omega)$ models the time-averaged energy contained in a narrow band around the frequencies of interest. Mathematically, this corresponds to

$$S_x(\omega) = \mathcal{F} \{ \Phi_x(\tau) \} \quad (10)$$

$$= \mathcal{F} \left\{ \lim_{t \rightarrow \infty} \frac{1}{t} \int_{-t/2}^{t/2} E \{ x(s + \tau) x(s)^* \} ds \right\}. \quad (11)$$

Using (1) and with $x_s(t) = \sum_{k=-\infty}^{+\infty} x_{s,k} e^{jk\omega_0 t}$ being the Fourier series corresponding to the oscillator's noise-free steady-state solution, where $\omega_0 = 2\pi/T$, the integral within the curly brackets can be approximated as

$$\Phi_x(\tau) \approx \sum_{k=-\infty}^{+\infty} |x_{s,k}|^2 e^{j\omega_0 k \tau} e^{-\frac{k^2 \omega_0^2 \sigma^2(\tau)}{2}}. \quad (12)$$

In obtaining (12), we made use of the fact that the process $\theta(t)$ varies slowly over time, i.e. on a time-scale T/ε . Moreover, we also used the result that the process $\theta(t + \tau) - \theta(t)$ is stationary and Gaussian with its variance $\sigma^2(\tau)$ determined from (7). The oscillator's output PSD is now found as the Fourier transform of (12) with respect to τ .

Finding the Fourier transform of (12) basically comes down to finding the Fourier transforms of

$$\Phi_{x,k}(\tau) = e^{-\frac{k^2 \omega_0^2 \sigma^2(\tau)}{2}} = e^{-\varepsilon^2 v_k(\tau)}. \quad (13)$$

In the expression above, the process $v_k(\tau) = k^2 \omega_0^2 \sigma^2(\tau) / (2\varepsilon^2)$ is introduced for convenience in further computations. It is solved from

$$\frac{d^2 v_k}{d\tau^2} = k^2 \omega_0^2 \Phi_{\bar{n}}(\tau), \text{ with } v_k(0) = 0, \frac{dv_k}{d\tau}(0) = 0. \quad (14)$$

In terms of the process $v_k(\tau)$, we then find

$$S_{x,k}(\omega) = \mathcal{F} \{ \Phi_{x,k}(\tau) \} \quad (15)$$

$$= 2 \int_0^{\infty} \cos(\omega\tau) e^{-\varepsilon^2 v_k(\tau)} d\tau \quad (16)$$

where we used the fact that $v_k(\tau) = v_k(-\tau)$ in obtaining (16). $S_{x,k}(\omega)$ represents the oscillator's normalized equivalent baseband phase noise spectrum (output PSD) around the k -th harmonic.

4. A GENERAL RELATION FOR OSCILLATOR PHASE NOISE SPECTRA

In a first step, we rewrite (16) in a manner that reveals the relation between the phase noise spectrum and the input noise PSD. This is of great help in gaining understanding on how the input noise characteristics affect the resulting oscillator spectrum. For weak input noise that varies sufficiently fast, i.e. for $\varepsilon \ll 1$ and $\tau_{noise} < T/\varepsilon$, it is even possible to obtain a single analytic expression that relates the noisy oscillator's output PSD to the input noise PSD. For input noise processes that do not satisfy these conditions, we resort to the numerical techniques discussed in section 5.

Integrating (16) by parts twice yields

$$S_{x,k}(\omega) = -\frac{2\varepsilon^2}{\omega^2} \int_0^{\infty} \left(\varepsilon^2 \left(\frac{dv_k}{d\tau} \right)^2 - \frac{d^2 v_k}{d\tau^2} \right) e^{-\varepsilon^2 v_k(\tau)} \times \cos(\omega\tau) d\tau. \quad (17)$$

In obtaining (17), we used the boundary conditions in (14). Furthermore, we assume that $S_{\bar{n}}(0) > 0$ such that, by virtue of (8), $\lim_{\tau \rightarrow \infty} v_k(\tau) = +\infty$. This in turn yields $\lim_{\tau \rightarrow \infty} e^{-\varepsilon^2 v_k(\tau)} = 0$. Using (14) and (16), (17) can be rewritten as

$$S_{x,k}(\omega) = -\varepsilon^4 \left(\frac{k^2 \omega_0^2}{2} S_{\bar{n}}(0) \right)^2 \frac{S_{x,k}(\omega)}{\omega^2} + \varepsilon^2 \frac{k^2 \omega_0^2}{\omega^2} (S_{\bar{n}}(\omega) + R_{x,k}(\omega)) \quad (18)$$

From this, we finally obtain

$$S_{x,k}(\omega) = \varepsilon^2 \frac{\frac{k^2 \omega_0^2}{\omega^2} (S_{\bar{n}}(\omega) + R_{x,k}(\omega))}{1 + \varepsilon^4 \frac{(k^2 \omega_0^2 S_{\bar{n}}(0)/2)^2}{\omega^2}}. \quad (19)$$

The residual term $R_{x,k}(\omega)$ in (18) and (19) equals

$$R_{x,k}(\omega) = \frac{2}{k^2 \omega_0^2} \int_0^{\infty} \left[\varepsilon^2 \left(\frac{k^2 \omega_0^2}{2} S_{\bar{n}}(0) \right)^2 e^{-\varepsilon^2 v_k(\tau)} - \varepsilon^2 \left(\frac{dv_k}{d\tau} \right)^2 e^{-\varepsilon^2 v_k(\tau)} + \frac{d^2 v_k}{d\tau^2} \left(e^{-\varepsilon^2 v_k(\tau)} - 1 \right) \right] \cos(\omega\tau) d\tau. \quad (20)$$

If this residual term is small compared to $S_{\bar{n}}(\omega)$, i.e. $|R_{x,k}(\omega)| \ll |S_{\bar{n}}(\omega)|$, (19) can be approximated as

$$S_{x,k}(\omega) \approx \varepsilon^2 \frac{k^2 \omega_0^2 S_{\bar{n}}(\omega)}{1 + \varepsilon^4 \frac{k^4 \omega_0^4}{4 \omega^2} \omega_0^2 S_{\bar{n}}(0)^2}. \quad (21)$$

We hence obtain a single analytical expression relating the oscillator's phase noise PSD to that of the driving noise processes. It is observed that the equivalent baseband PSD $S_{x,k}(\omega)$ is that of the filtered averaged input noise signal $\varepsilon \bar{n}(t)$. The filter is a first-order low-pass filter with a DC gain and corner frequency that depend on the properties of the input noise process.

It is important to remind that (21) is only valid when the term $R_{x,k}(\omega)$ in (19) can be neglected. A practical criterion for delimiting those noise sources for which this is satisfied is given by the inequality

$$\kappa \varepsilon^2 S_{\bar{n}}(0) \tau_{noise} \ll \frac{2}{k^2 \omega_0^2}. \quad (22)$$

Observing (22), it is seen that the approximation (21) breaks down when either the noise strength ε , the normalized input noise PSD DC-level $S_{\bar{n}}(0)$ or the noise time constant τ_{noise} grow large. Put differently, (21) breaks down when the input noise grows strong or when it varies very slowly over time.

As a final note: if we consider the asymptotic behavior of (21) for ω becoming large, i.e. for $\omega > \varepsilon^2 k^2 \omega_0^2 S_{\bar{n}}(0)/2$, then we obtain

$$S_{x,k}(\omega) \approx \varepsilon^2 k^2 \frac{\omega_0^2}{\omega^2} S_{\bar{n}}(\omega). \quad (23)$$

This expression is consistent with the well-known $1/\omega^2$ and $1/\omega^3$ characteristics for respectively white input noise ($S_{\bar{n}}(\omega) \sim 1$) and $1/f$ input noise ($S_{\bar{n}}(\omega) \sim 1/\omega$). It is readily shown that the asymptote (23) corresponds with the one presented in [3]. The same holds for the asymptotic behavior as $\omega \rightarrow 0$. Also, for a white noise input, the expression (21) becomes exact and coincides with the Lorentzian spectrum discussed in [3, 4].

5. NUMERICAL PHASE NOISE SPECTRUM COMPUTATION

When the noise level ε gets large or when the noise is of a slow-varying type, i.e. when (22) is no longer satisfied, the approximation (21) is no longer valid. This especially holds true for small frequency offsets. Situations like this may arise in dealing with $1/f$ input noise processes. For such cases, we propose the numerical computation of the residual term $R_{x,k}(\omega)$ in (19) in order to obtain a more accurate result. The procedure to do so goes as follows:

1. In (20), evaluate the terms in the square brackets and fit them using complex exponential basis functions, i.e. find a set of $A_m \in \mathbb{C}$ and $z_m \in \mathbb{C}$ such that

$$\begin{aligned} r_{x,k}(\tau) = \varepsilon^2 & \left(\frac{k^2 \omega_0^2}{2} S_{\bar{n}}(0) \right)^2 e^{-\varepsilon^2 v_k(\tau)} \\ & - \varepsilon^2 \left(\frac{dv_k}{d\tau} \right)^2 e^{-\varepsilon^2 v_k(\tau)} \\ & + \frac{d^2 v_k}{d\tau^2} \left(e^{-\varepsilon^2 v_k(\tau)} - 1 \right) = \sum_m A_m e^{z_m \tau}. \end{aligned} \quad (24)$$

Use of an exponential fit helps avoiding trouble that arises due to truncating the numerical evaluation of $r_{x,k}(\tau)$ to a finite window of time. The right-hand side sum of exponentials always provides a smooth extrapolation towards infinity.

2. Substitute the exponential fit (24) back into (20). It is then straightforward to obtain

$$\begin{aligned} R_{x,k}(\omega) &= \frac{2}{k^2 \omega_0^2} \int_0^\infty r_{x,k}(\tau) \cos(\omega \tau) d\tau \\ &= -\frac{2}{k^2 \omega_0^2} \sum_m A_m \frac{z_m}{\omega^2 + z_m^2}. \end{aligned} \quad (25)$$

In what follows, we provide some details on how the procedure above is implemented. Focus is given to the case where the input noise process $\bar{n}(t)$ is a combination of white and $1/f$ noise.

5.1 Modeling the input noise process

In order to evaluate $r_{x,k}(\tau)$, we need a set of models that allow capturing input noise behavior. In what follows, we assume the —normalized— input noise process $\bar{n}(t)$ to be a combination of white and $1/f$ (flicker) noise. The autocorrelation function of such a noise process can be modeled as

$$\Phi_{\bar{n}}(\tau) = \delta(\tau) + 2f_{1/f} E_1(\gamma|\tau|). \quad (26)$$

where $E_1(t) = \int_1^\infty (e^{-z}/z) dz$ represents the exponential integral. The meaning of the parameter γ will be made clear soon. The first term in (26) is a Dirac Delta function capturing white noise effects while the second term represents the autocorrelation function of the stationary $1/f$ noise model presented in [2, 3]. Furthermore, $f_{1/f}$ is the input noise $1/f$ corner frequency, i.e. the frequency (in Hz) beyond which the PSD of the $1/f$ input noise drops below the white noise level. The autocorrelation function (26) corresponds to the PSD

$$S_{\bar{n}}(\omega) = 1 + f_{1/f} \frac{2\pi}{|\omega|} \left(1 - \frac{2}{\pi} \arctan \left(\left| \frac{\gamma}{\omega} \right| \right) \right). \quad (27)$$

From this expression for $S_{\bar{n}}(\omega)$, it is observed that the parameter γ represents the frequency whereby, for $\omega \rightarrow 0$, the $1/f$ noise characteristic goes over into a flat one with $S_{\bar{n}}(0) = 1 + 4f_{1/f}/\gamma$.

5.2 Fitting $r_{x,k}(\tau)$

Given the noise model, we compute $r_{x,k}(\tau)$ for $\tau \in [0, \tau_c]$. To do so, we solve (14) for $v_k(\tau)$ and $dv_k/d\tau$ and substitute the results in (24). Furthermore, τ_c is the time for $r_{x,k}(\tau)$ to become sufficiently small. Typical values for τ_c tend to be proportional to the time constant τ_{noise} characterizing the input noise. Having computed $r_{x,k}(\tau)$, we determine the coefficients A_m and the exponents z_m of the exponential fit in the right-hand side of (24) using a Hankel Total Least Squares (HTLS) algorithm [9]. The algorithm takes a set of N equidistant samples $r_{x,k}(n\tau_c/(N-1))$ as an input and produces the desired A_m and z_m . The number of samples N is determined by the maximum frequency $\omega_{FIT} \approx 2\pi N/\tau_c$ for which one wants the spectrum of the fit to correspond with the actual spectrum $\mathcal{F}\{r_{x,k}(\tau)\} = k^2 \omega_0^2 R_{x,k}(\omega)$. This choice is driven by the requirement that $|R_{x,k}(\omega)| \ll |S_{\bar{n}}(\omega)|$ for $\omega > \omega_{FIT}$. Experiments show this to be satisfied for ω_{FIT} larger than the corner frequency of the denominator in (21), or

$$\omega_{FIT} \approx 2\pi \frac{N}{\tau_c} \sim \varepsilon^2 \frac{k^2 \omega_0^2}{2} S_{\bar{n}}(0). \quad (28)$$

With (27) this implies that $N \sim \varepsilon^2 k^2 \omega_0^2 \frac{f_{1/f} \tau_c}{\gamma}$. Hence, as γ grows small, N grows large. Since the complexity of the HTLS algorithm roughly grows with N^3 , a lower bound is imposed on γ by reasons of limiting computational complexity. Typically, however, this bound is low enough to yield valuable results on the shape of an oscillator's phase noise spectrum.

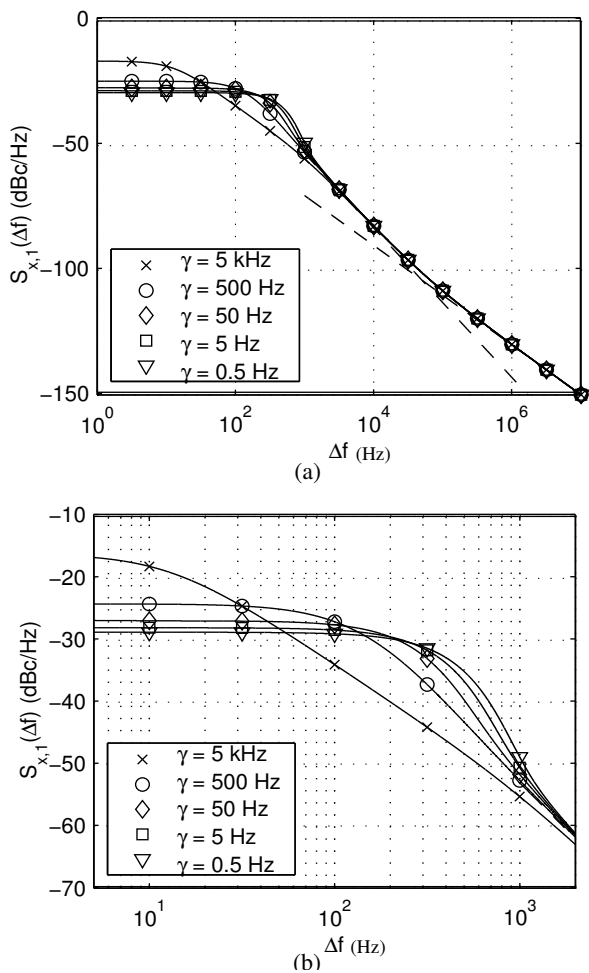


Figure 1: Phase noise spectrum $S_{x,1}(\Delta f)$ around carrier frequency. The spectrum is shown for different values of γ . The upper figure shows the entire spectrum while the lower figure zooms in on the close-in phase noise characteristic.

6. RESULTS

The algorithm above was implemented in Matlab and takes 15-30 seconds to execute on a Pentium IV. All tests were accomplished for a noise strength $\epsilon = \sqrt{1e-19}$. Furthermore, the autocorrelation function of the normalized input noise $\bar{n}(t)$ was modeled as in (26) with $f_{1/f} = 50$ kHz. The oscillation frequency was set to $f_0 = 1$ GHz. The numbers above roughly result in a phase noise spectrum valued -130 dBc/Hz at 1 MHz and with a $1/f^3$ corner frequency at 50 kHz.

Fig. 1 shows $S_{x,1}(\Delta f)$, modeling the phase noise spectrum near the oscillation frequency f_0 . This spectrum was computed for values of γ ranging from 0.5 Hz to 5 kHz. Here, γ is the low-frequency corner in the input noise $1/f$ PSD modeled by the second term in (27). As can be seen, for small values of γ , the very close-in phase noise spectrum flattens and there is a steep edge making the transition from the DC-level to the traditional $1/f^3 - 1/f^2$ characteristic. The corner of this edge is, for this example, located near 300 Hz. For frequency offsets beyond 1 kHz, the spectrum assumes a $1/f^3$ shape. Furthermore, as γ decreases, the close-in phase noise characteristic shows a dropping DC-level and an increasing corner frequency. With regard to these observations, elementary theoretic

considerations have lead us to believe that the DC-level keeps dropping in a manner that becomes proportional to $|\ln(\gamma)|$ while the corner frequency increases like $|\ln(\gamma)|$.

The low frequency corner appearing in Fig. 1 makes good sense when considering the fact that the total energy contained underneath the —normalized— spectrum $S_{x,1}(\Delta f)$ equals 1, i.e.

$$\int_{-\infty}^{+\infty} S_{x,1}(\Delta f) d\Delta f = \frac{1}{2\pi} \int_{-\infty}^{+\infty} S_{x,1}(\omega) d\omega = 1 \quad (29)$$

If, for a given Δf_c ,

$$S_{x,1}(\Delta f_c) \approx \epsilon^2 \frac{f_0^2}{\Delta f_c^2} S_{\bar{n}}(\Delta f_c) \quad (30)$$

holds valid, it is readily shown that

$$1 = \int_{-\infty}^{+\infty} S_{x,1}(\Delta f) d\Delta f \geq \epsilon^2 2 \frac{f_0^2}{\Delta f_c} S_{\bar{n}}(\Delta f_c) \quad (31)$$

This implies that the validity of (30) must break down before the right-hand side of (31) exceeds 1. Assuming this to happen for a frequency Δf_c below f_1/f , it then holds that $\Delta f_c \geq \epsilon f_0 \sqrt{2} f_1/f$. For our example, this yields $\Delta f_c \geq 100$ Hz which is in agreement with the results in Fig. 1.

7. CONCLUSIONS

This paper has presented a generalized semi-analytic method for computing oscillator phase noise spectra, including the details very close to the oscillation frequency. The method is based on a general relation between the oscillator phase noise spectrum and the input noise characteristics. For weak input noise processes that vary sufficiently fast over time, this relation reduces to a single analytic expression. For cases that do not satisfy the above conditions, the relation is, in part, evaluated numerically using exponential data fitting techniques. Phase noise spectra as computed for a combination of white and $1/f$ input noise show a close-in phase noise spectrum that flattens near the oscillation frequency with a steep edge making the transition to the traditional $1/f^3 - 1/f^2$ characteristic. This behavior, however, typically occurs for very small frequency offsets. For large frequency offsets, the phase noise spectrum assumes the well-known $1/f^3 - 1/f^2$ characteristic.

8. REFERENCES

- [1] M. Keshner, "1/f Noise", In Proc. of the IEEE, vol. 70, nr. 3, pp. 212-218
- [2] F.X. Kaertner, "Analysis of White and $f^{-\alpha}$ Noise in Oscillators", In *Int. J. Circuit Theory Appl.*, vol. 18, pp 485-519, 1990
- [3] A. Demir, "Phase Noise in Oscillators: DAEs and Colored Noise Sources", In Proc. *IEEE/ACM ICCAD*, pp. 170-177, San Jose, 1998
- [4] A. Demir, A. Mehrotra and J. Roychowdhury, "Phase Noise in Oscillators: A Unifying Theory and Numerical Methods for Characterization", In *IEEE Trans. Circ. and Syst.-I*, vol. 47, no. 5, pp. 655-674, May 2000
- [5] A. Hajimiri and T.H. Lee, "A General Theory of Phase Noise in Electrical Oscillators", In *IEEE J. Solid-State Circ.*, vol. 33, no. 2, pp. 179-194, February, 1998
- [6] P. Vanassche, G. Gielen and W. Sansen, "On the Difference Between Two Widely Publicized Methods for Analyzing Oscillator Phase Behavior", In Proc. *IEEE/ACM ICCAD*, Session 4A, San Jose, 2002
- [7] J.A. Mullen and D. Middleton, "Limiting Forms of FM Noise Spectra", In Proc. of the IRE, vol. 45, no. 6, pp. 874-877, June, 1957
- [8] D. Middleton, *Statistical Communication Theory*, Peninsula Publishing, Los Altos, California, 1987
- [9] S. Van Huffel, C. Decanniere, H. Chen and P. Van Hecke, "Algorithm for Time-Domain NMR Data Fitting Based on Total Least Squares", In *Journal of Magnetic Resonance A*, vol. 110, pp. 228-237, 1994.